Atomic diffusion and band lineups at $In_{0.53}Ga_{0.47}As$-on-InP heterointerfaces

P. E. Smith[a)]
Department of Physics, The Ohio State University, Columbus, Ohio 43210

S. H. Goss, M. Gao, M. K. Hudait, and Y. Lin
Department of Electrical and Computer Engineering, The Ohio State University, Columbus, Ohio 43210

S. A. Ringel and L. J. Brillson
Department of Physics and Department of Electrical and Computer Engineering,The Ohio State University, Columbus, Ohio 43210

(Received 3 March 2005; accepted 23 April 2005; published 25 July 2005)

We have used secondary ion mass spectrometry (SIMS), cathodoluminescence spectroscopy (CLS), and an analysis of secondary electron thresholds (SETs) to determine how extended anion soaks during molecular beam epitaxial (MBE) growth transitions affect band lineups at the lattice-matched $In_{0.53}Ga_{0.47}As$-on-InP interface. Growth transitions consisting of 20–150 As soaks result in SIMS-measured interfacial broadening of up to 8 nm. By monitoring SETs across an *in situ* cleaved InP/$In_{0.53}Ga_{0.47}As$/InP double heterostructures, we measure a type I conduction-band offset of 190 ± 30 meV at an abrupt InGaAs-on-InP interface. For diffused structures exposed to long As soak times, we observe an effective decrease of ΔE_c by up to 210 ± 40 meV. The changes in InGaAs and InP CL intensities are consistent with both the SET-measured decrease in conduction-band offset and an increase in nonradiative recombination at the diffused InGaAs-on-InP interface. © *2005 American Vacuum Society.* [DOI: 10.1116/1.1949218]

I. INTRODUCTION

The $In_xGa_{1-x}As$/InP system has been the focus of intense research owing to its application in infrared photodetectors and active electrons such as high-speed bipolar junction transistors. The system is especially useful as an optoelectronic material because the band gap (1.55 μm) of the lattice-matched composition ($x=0.53$) corresponds to a well in the absorption spectrum of silica fibers. InGaAs/InP growth remains difficult because both cation and anion sources switch during growth transitions. To maintain the high anion to cation beam pressure ratio necessary for two-dimensional growth during a transition from one semiconductor to another, an anion "soak" (i.e., anion exposure without growth) is usually employed to allow the new anion pressure to equilibrate in the chamber prior to the growth of subsequent layers. During an As soak at the InGaAs-on-InP interface, the replacement of several monolayers of P by As, due to an exchange reaction, has been widely reported.[1–4] Subsequent exposure to P has been shown to eliminate As and restore the InP surface; however, immediately starting InGaAs growth after As exposure results in a trapping of As atoms in the recently grown InP layer.[5] Longer As exposures, particularly at high temperatures, have been shown to result in increased As incorporation in the InP lattice, leading to interfacial roughening as strained InAsP layers or islands form.[6–10] Such a change in interface microstructure might well affect interface-related optical and electrical properties. Indeed, an extended As soak has been shown to result in broadened near-band-edge (NBE) cathodoluminescence emission at InGaAs/InP interfaces and correspondingly to alter the performance of single quantum well structures.[10,11] Electrically, an extended As soak has been shown to increase carrier lifetimes measured by photoconductive decay (PCD) due to an As-defect related persistent photoconductivity.[12] These growth-transition-related effects are not restricted to the InGaAs/InP system. A dependence of interface quality and charge density on As soak time in InGaP/GaAs heterostructures, where both anion and cation sources change during growth and an As–P exchange mechanism operates, has been reported.[13,14]

II. EXPERIMENT

The structures used in this study are five nominally ($n\sim10^{15}$ cm^{-3}) undoped, lattice-matched, InP/$In_{0.53}Ga_{0.47}As$/InP double heterostructures (DHs) grown on semi-insulating Fe-doped (100) InP substrates with no ($<\pm0.2^0$) miscut by solid source molecular beam epitaxy (MBE) with valved cracker sources for arsenic and phosphorus. Prior to being loaded into the growth chamber, epiready InP wafers are subject to a 60 min. 300 °C anneal under a pressure of 5×10^{-9} Torr to remove water vapor. Substrate oxide desorption is done in the growth chamber at a temperature 510 °C under a P overpressure of 1×10^{-5} Torr. The observed (2×4) reflection high energy electron diffraction (RHEED) pattern indicates a clean (100) InP surface. After oxide desorption, growth takes place at 485 °C using group-V to group-III beam pressure ratios of 24:1 for InGaAs and 12:1 for InP. Growth rates are 1.743 and 3.180 A/s for InP and InGaAs, respectively. Figure 1 shows a growth diagram for the five DHs. Beginning at the substrate, the layers are: 200 nm InP, 500 nm $In_{0.53}Ga_{0.47}As$, and 50 nm

[a)]Author to whom correspondence should be addressed; electronic mail: psmith@fox.mps.ohio-state.edu

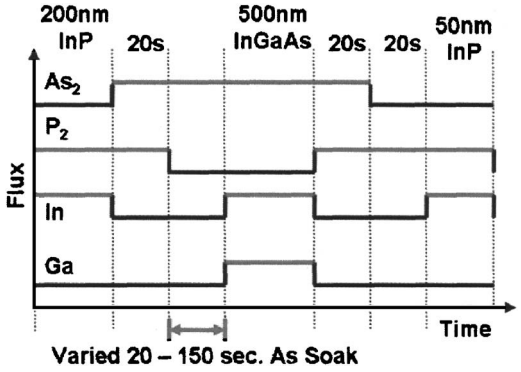

FIG. 1. MBE growth diagram for the five InP/$In_{0.53}Ga_{0.47}As$/InP DHs studied. The As soak time at the InGaAs-on-InP interface varies from 20 to 150 s.

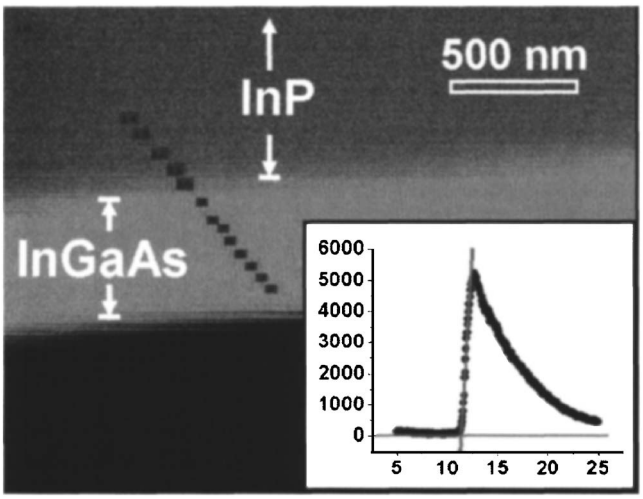

FIG. 2. SEM image showing SET analysis spots along a line angled to the InGaAs-on-InP interface. The intensity vs energy plot in the inset shows a representative SET measurement at a single point.

InP. Arsenic soak times at the InGaAs-on-InP interface, defined as the length of time that As is allowed to soak on the 200 nm InP surface after the P source is closed and prior to InGaAs growth, are 20, 60, 90, 120, and 150 s for the five structures. The (2×4)-fold RHEED pattern remains stable during As_2 exposure on the 200 nm InP layer for all five structures. This indicates consistent conditions for the growth of subsequent layers.

Negative-ion secondary ion mass spectrometry (SIMS) is performed on a PHI (TRIFT-III TOF SIMS with a background pressure during analysis of 2×10^{-9} Torr. For depth profiling, a 1 keV Cs^+ beam is used as a sputter source. The analysis beam is a 15 keV, isotopically pure, focused ^{69}Ga ion beam. Typical depth profiling time is approximately 1 h/sample. The sputter depth rates vary by up to 50% from profile to profile. In order to compare depth profiles of intensity versus sputter depth, we normalize the depth scales to the onset of the As profile decrease from its bulk value at the InGaAs-on-InP interface. The normalized profiles provide a relative measure of interface broadening.

We used an ultrahigh vacuum (UHV) scanning electron microscope (SEM) to measure the secondary electron thresholds (SETs) (i.e., the vacuum level energy E_{VAC} relative to the Fermi level E_F) and hence the work function changes across the InGaAs/InP heterojunction in cross section. Previously Sakai *et al.*[15] used a similar technique to measure metal work functions. The linear edge of the SET in an intensity versus energy plot extrapolated to the baseline yields the energy onset. This onset represents the difference in semiconductor and analyzer work functions. In our study we apply a -12 V bias to the sample so that all emitted electrons are collected by the energy analyzer.[15] As in the Sakai study, we perform SET measurements using a JEOL JAMP-7800F UHV SEM as the electron excitation source. Changes in the surface Fermi level position due to contamination or Fermi level pinning will change the local SET measurement. To minimize these effects, heterostructures are cleaved *in situ* to yield a clean, unpinned, (011) surface.[16] To promote cleavage along the (011) surface, we score the substrate (i.e., the nongrowth surface) with a diamond scribe before moving the sample to the SEM processing and analysis chambers. Cleave quality is initially assessed in the SEM. Because the SEM-observed secondary electron intensity is sensitive to changes in work function on the sub-10 nm scale,[17–19] cleave artifacts which could significantly affect the surface potential distribution can be imaged and avoided. Structures that show significant evidence of cleave-related damage in the interface region of interest are discarded. The incident 5 keV electron beam current is a constant 1 nA for all SET measurements. A hemispherical energy analyzer attached to the UHV SEM measures the ejected secondary electron energies. At the $80\,000\times$ SEM magnification used for our measurement, beam-positioning resolution is approximately 50 nm. This is small relative to the micron-scale space charge regions in these nominally undoped structures. With a semiconducting sample, the bias and analyzer work function remain constant while the semiconductor work function changes with the E_F position in the band gap. Thus SETs measure the semiconductor vacuum-level energy E_{VAC} with a constant offset. Subtracting literature values for InGaAs and InP election affinities,[20] which are assumed to be constants in the bulk semiconductors, from the E_{VAC} data yields the conduction-band edge in the region of electron beam excitation. Therefore, we measure the associated band offset by monitoring SETs as the incident electron beam is moved across the InGaAs-on-InP interface.

Figure 2 shows a SEM image of an *in situ* cleaved structure with analysis positions along a line angled to the interface. The inset shows the linear onset of a single SET analysis point that is extrapolated to the baseline to determine E_{VAC}. The square points denote the set of measurement positions for a single profile. We collected similar profiles across the InGaAs-on-InP interface at several positions for each heterojunction. Each profile required approximately 20 min. Auger electron spectroscopy verified the surface cleanliness before and after each series of profiles.

We also obtained cathodoluminescence (CL) spectra in plan view using the JEOL SEM with a liquid helium cold

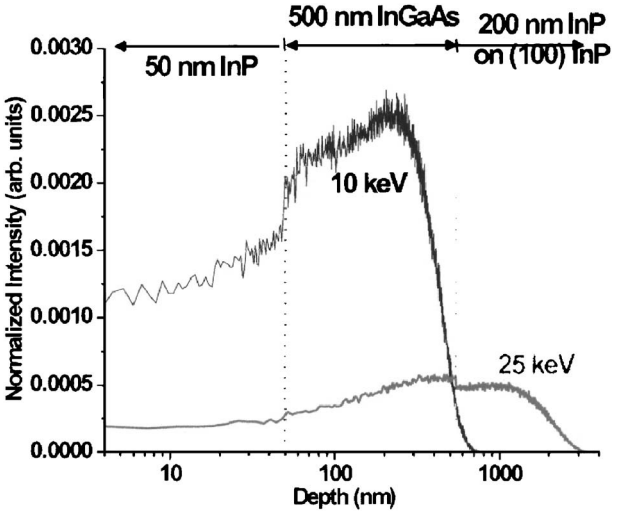

FIG. 3. Primary electron depth penetration for 10 and 25 kV beam energies showing selective excitation of the InGaAs and InP layers, respectively.

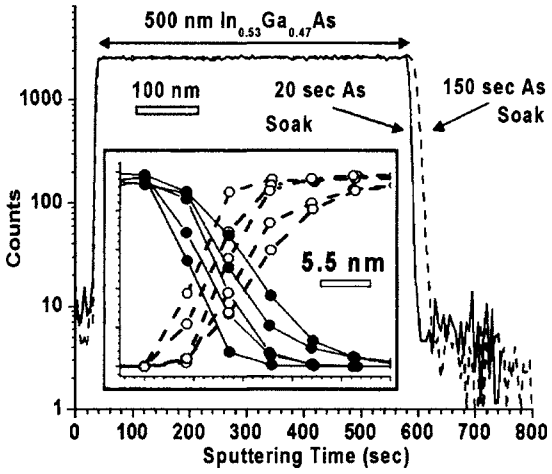

FIG. 4. SIMS depth profiles showing broadening at the InGaAs-on-InP interface in structures exposed to 20 (solid line) and 150 s (dashed line) As soaks. The profiles show no difference in broadening at the outer InP-on-InGaAs control interface. The inset shows monotonic InGaAs-on-InP interface broadening in As (filled circles with solid line) and P (open circles with dashed line) SIMS profiles for all five structures.

stage at 10 K to improve the signal-to-noise analysis. The optical train consisted of an Oxford MonoCL system with a parabolic mirror set in UHV and focused light collection through a sapphire window at the vacuum-air interface along with an Edinburgh Instruments high-purity germanium detector. Incident beam energies were 10 and 25 kV with currents of 1 and 20 nA, respectively, with the electron beam rastered over a 100 μm^2 area and spectral resolution was <1 nm. Incident electron beams with increasing energies create electron-hole pairs that recombine at increasing depths, with characteristic spectra. Figure 3 illustrates Monte Carlo simulations showing primary electron excitation depth and distribution versus beam energy.[21] For a 10 keV incident beam, the simulations show that approximately 90% of primary electrons penetrate into the 500 nm InGaAs layer but not into the 200 nm InP layer. Approximately 75% of the higher energy, 25 keV, electrons are able to penetrate the InGaAs-on-InP interface into the 200 nm InP and substrate layers.

III. RESULTS

Figure 4 shows SIMS As depth profiles for structures exposed to 20 and 150 s As soaks. We assume that the 20 s soaked structure is atomically abrupt and that the observed 8.5 nm broadening is a result of the sputter process at the 550 nm profiling depth. We define the interface width as the distance over which the SIMS-measured As intensity changes from 90% to 10% of its bulk value. Thus, Fig. 4 indicates an additional broadening of 8 nm for the most diffused, 150 s soaked, structure. Both profiles are abrupt at the InP-on-InGaAs control interface to within the 7.5 nm sputter-induced broadening of the SIMS at the 50 nm profiling depth. The Fig. 4 inset shows InGaAs-on-InP interface As and P profiles for all five structures. Arsenic and P profiles broaden monotonically with increasing As soak at the InGaAs-on-InP interface.

Figure 5 displays one representative cross-sectional SET measurement for each of the five structures (soak times). Energy error bars are calculated from the intersection of the 2σ confidence bands with the baseline. Using a Monte Carlo simulation[21] to calculate the surface radius of backscattered electrons, we estimate that 95% of the secondary electrons are ejected from the surface within 125 nm of the incident electron beam. This "interface region" corresponds to the shaded region of Fig. 5. The change in SET as the primary electron beam is moved from InGaAs into InP corresponds to the change in E_{VAC} relative to E_F across the interface region.

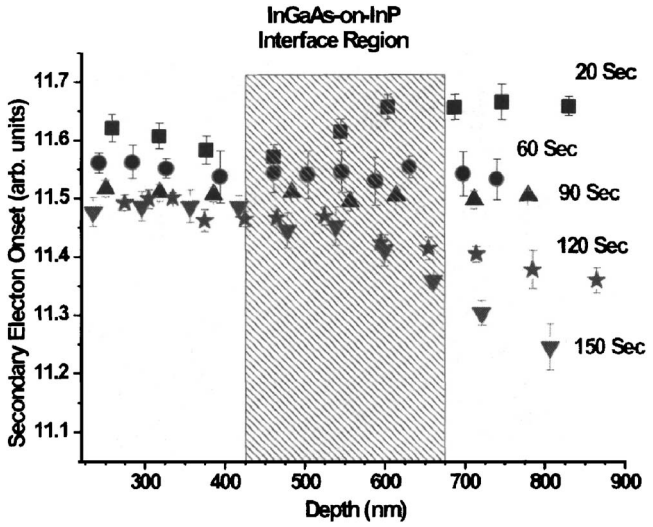

FIG. 5. SET measurements performed on the *in situ* cleaved (011) surface for all five DHs. The shaded region corresponds to the region over which interface specific changes are expected to occur under SEM electron beam bombardment.

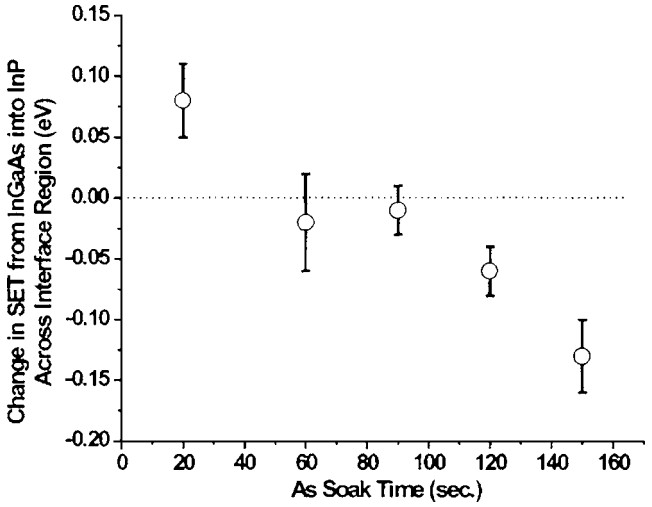

FIG. 6. Total change in SET vs electron beam position across the InGaAs-on-InP interface region from InGaAs into InP for the different As soak times. The dashed line corresponds to $\Delta E_c = 0$.

The set of SET profiles indicates that the relative work function change from InGaAs to InP decreases with increasing As soak time.

Figure 6 summarizes the changes in SET across the interface region. Each data point represents an average of the SET-measured change across the interface region at multiple positions on the (011) face of each structure. The corresponding points and their associated error bars are averaged, with each data point assigned unity weight, to obtain the error bars shown. Figure 6 shows that the average SET measured from InGaAs into InP increases by 80±30 meV for the most abrupt structure with only a 20 s As soak. On the other hand, the SET decreases by 130±30 meV for the diffused structure with a 150 s soak. The SET profiles exhibit intermediate changes between these two soak time extrema. Figure 6 displays a near-monotonic, almost linear, relationship between As soak time and cross sectional change in SET and a total change of −210±40 meV between samples with 20 and 150 s As soak time.

Integrated intensities of NBE emissions measured in plan view at 10 K provide a measure of the radiative recombination within the InGaAs and InP layers for each heterojunction. Figure 7 shows (a) the integrated 10 keV InGaAs NBE emission and (b) the integrated 25 keV InP to InGaAs (InP/InGaAs) NBE emission ratio plotted versus As soak time. The 10 keV result is a measure of the total radiative recombination occurring via InGaAs NBE states. The 25 keV ratio provides a relative measure of radiative recombination via NBE transitions occurring in the InP versus InGaAs regions. The InP signal is too low for a similar ratio comparison at 10 kV beam energy due to the small amount of recombination occurring in the InP for 10 keV electrons, as indicated in Fig. 3, and the ~80% absorption of ~1.41 eV InP NBE emissions in the 500 nm InGaAs layer. Error bars correspond to 1 s.d. from the mean of multiple data points for each structure. The 10 keV results show a decrease in integrated NBE intensity of approximately 30%–35% as As soak time increases from 20 to 150 s. The 25 keV ratio shows a similar decrease.

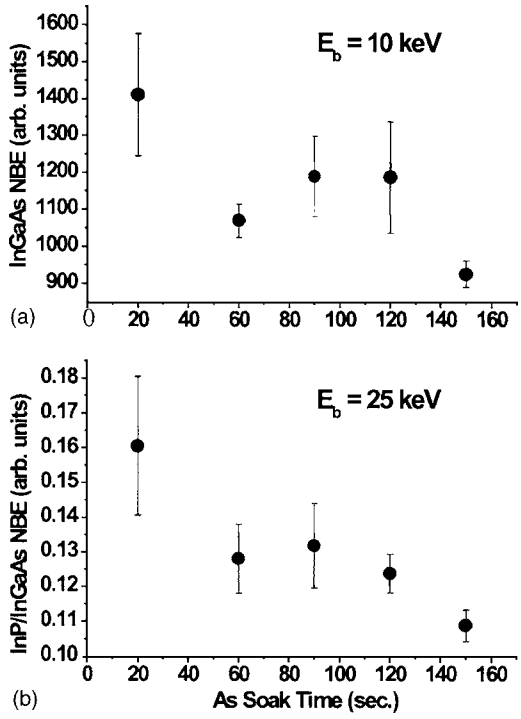

FIG. 7. Integrated CLS peak intensity of: (a) 10 keV InGaAs NBE and (b) 25 keV InP to InGaAs NBE ratio vs As soak time, showing effects of band offset changes.

IV. DISCUSSION

The considerable SIMS-observed broadening shown in Fig. 4 is indicative of As diffusion into the 200 nm InP buffer layer during growth. An As–P exchange reaction proposed to explain As incorporation in the InP layer would, in the case of diffusion during an As soak, result in the desorption of P into the vacuum and does not alone explain the observed broadening of the P profiles. Our observation of the broadening of P as well as the As profile could be related to the highly reactive nature of P with Ga. This is supported by the observation of Ga–P bonding at the InGaAs-on-InP interface by several authors.[11,22,23] Alternatively, the diffusion of some As atoms via a kickout or similar interstitial-based mechanism could leave mobile P atoms free to diffuse back into the InGaAs layer, leading to P-profile broadening.

SET measurements probe electronic band structure changes associated with the SIMS-measured broadening at the InGaAs-on-InP interface. The measured vacuum level minus the electron affinity on each side of the heterojunction yields a conduction-band profile with a constant offset due to the applied bias and analyzer work function. Bulk electron affinity values[20] are: $\chi(\mathrm{InP}) = 4.40$ and $\chi(\mathrm{In_{0.53}Ga_{0.47}As}) = 4.51$ from a Vegard's law interpolation between $\chi(\mathrm{GaAs}) = 4.07$ and $\chi(\mathrm{InAs}) = 4.90$. Figure 8 qualitatively illustrates how ΔE_c is extracted from SET data via electron affinities. Our measured ΔE_{VAC} of 80±30 meV for the abrupt, 20 s

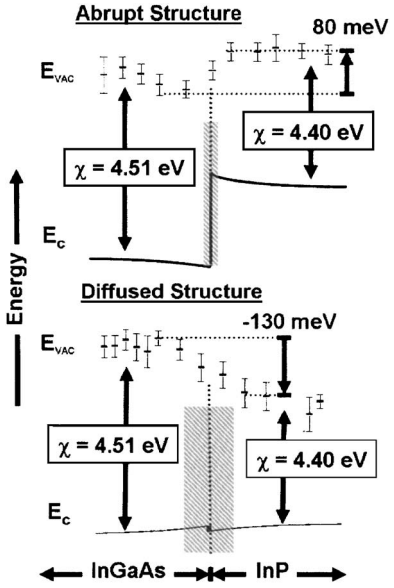

FIG. 8. SET measurements for abrupt (20 s) and diffused (150 s) structures. Subtracting bulk electron affinities yields a conduction-band profile with corresponding conduction-band offset.

soaked, structure corresponds to a ΔE_c of 190±30 meV after subtracting the bulk electron affinities. This compares favorably with the capacitance-voltage measured literature value[24] of 230 meV and confirms the accuracy of our technique. The slight underestimate of our measurement is likely due to the limit on how close the beam can be positioned to the InGaAs-on-InP interface imposed by a 15 nm beam diameter (for a 5 kV, 1 nA analysis), primary electron scattering, and sample drift during analysis. For the most diffused structure, exposed to a 150 s As soak, we observe a ΔE_{VAC} of −130±30 meV. This ΔE_{VAC} corresponds to a ΔE_c of −20±30 meV. Intermediate soak times exhibit intermediate decreases in ΔE_{VAC} and corresponding ΔE_c. Thus, a decrease in the change in SET across the interface region from InGaAs into InP with increasing As soak time is consistent with an effective lowering of the conduction-band offset ΔE_c in diffused samples exposed to long As soaks.

The cathodoluminescence data shown in Fig. 7 support a decrease in ΔE_c in the more diffuse structures. Since the excitation depth (beam energy) is constant, any changes in NBE emission intensity with As soak time are due to changes in either carrier diffusion between layers or radiative recombination via NBE states. The conduction- and valence-band offsets at the InGaAs-on-InP interface in the abrupt structures are barriers to carrier diffusion from the InGaAs into the InP. In the case of incident 10 keV electrons, which predominantly create electron-hole pairs in the InGaAs region, conduction-band electrons are more easily able to cross the lowered ΔE_c barrier into the InP region in the diffuse structures. This accounts for a decrease in InGaAs NBE intensity with increasing As soak time. Similarly, *n*-type band bending for the 200 nm InP buffer layer in the most abrupt heterojunction represents a barrier to electron diffusion from the InP into the InGaAs. The 25 keV incident beam creates electron-hole pairs predominantly in the 200 nm InP buffer layer and conduction-band electrons are able to cross more easily into the InGaAs in the more diffuse junctions. This leads to a decrease in InP NBE intensity relative to InGaAs.

A decrease in effective band offset can be a result of internal strain, chemical interlayers, interface charges, or defects which alter the interface dipoles that determine band offsets. Hudait *et al.*[12] have presented PCD evidence of an As defect-related trap at the InGaAs-on-InP interface which is associated with long As soak times in these structures. Our 10 kV CLS measurements showing a ~35% decrease in the measured InGaAs NBE intensity in structures exposed to long As soaks are consistent with a decrease in radiative recombination, possibly as a result of this interface trap. If interface trapping accounts for the measured decrease we also expect some of the carriers diffusing from InP back into InGaAs to recombine nonradiatively, particularly in the structures exposed to longer soak times. The decrease in 25 kV InP/InGaAs NBE intensity with increasing As soak time shows that a change in band offset is the dominant interface effect. If interface states were dominant (as opposed to a change in effective band offset) an increase in the InP/InGaAs ratio would be expected due to less radiative InGaAs emission in the diffused structures exposed to longer soak times. Thus, while our results are consistent with an increase in nonradiative recombination via an increase in interface state density, nonradiative states at the interface do not alone account for the monotonic dependence of relative NBE recombination in Fig. 7(b).

Strained interlayers could also modify the effective band offset. Several authors have reported compressively strained InAsP layers or islands at the InGaAs-on-InP interface.[6–10] This has been reported in the $InAs_{1-x}P_x/In_{0.53}Ga_{0.47}As_{1-y}P_y$ system where experimentally measured changes in band lineup are attributed to compositional changes and strain development at the heterointerface.[25] It has been shown that InAsP on (100) InP exhibits a (2×4)-fold RHEED pattern similar to (100) InP;[26] therefore, the stable (2×4)-fold RHEED pattern exhibited during As exposure at the InGaAs-on-InP interface does not preclude the possibility of a strained interlayer. A thinner interfacial layer is expected to change the band offset less as the wave functions of states in the InGaAs and InP layers can penetrate the thin interlayer and play a larger role in determining the band offset. This could account for the monotonic changes observed with As soak time.

V. CONCLUSION

We have directly measured the heterojunction band offset across UHV-cleaved InGaAs-on-InP interfaces in cross section using localized work functions obtained from secondary electron thresholds. The conduction-band offset measured for an abrupt junction, involving a 20 s As soak, was 190±30 meV, consistent with previous measurements. With increasing As soak time, the heterojunction exhibits anion interdiffusion and broadening as measured by SIMS, extending up to 8 nm for a 150 s As soak. Associated with this

increased broadening is a 210±40 meV decrease in the effective conduction-band offset. Depth-dependent CL spectra show monotonic changes in InGaAs versus InP light emission with increasing As soak time that are consistent with increased electron flow across the reduced conduction-band offset and band bending as well as reduced intensities overall that are consistent with interface charge trapping. Overall, these results demonstrate that atomic interdiffusion associated with growth transitions can have considerable effects on the electrical properties of a lattice-matched III–V heterojunction.

ACKNOWLEDGMENTS

This work is supported by the Department of Energy (Jane Zhu), the National Science Foundation (Verne Hess), and the Office of Naval Research (Colin Wood).

[1]J. M. Moison, M. Bensoussan, and F. Houzay, Phys. Rev. B **34**, 2018 (1986).
[2]G. Hollinger, D. Gallet, M. Gendry, C. Santinelli, and P. Victorovitch, J. Vac. Sci. Technol. B **8**, 832 (1990).
[3]C. H. Li, L. Li, D. C. Law, S. B. Visbeck, and R. F. Hicks, Phys. Rev. B **65**, 205322 (2002).
[4]B. X. Yang, L. He, and H. Hasegawa, J. Electron. Mater. **25**, 379 (1996).
[5]D. E. Aspnes, M. C. Tamargo, M. J. S. P. Brasil, R. E. Nahory, and S. A. Schwartz, Appl. Phys. Lett. **64**, 3279 (1994).
[6]D. C. Law, Y. Sun, C. H. Li, S. B. Visbeck, G. Chen, and R. F. Hicks, Phys. Rev. B **66**, 045314-1 (2002).
[7]J. Decobert and G. Patriarch, J. Appl. Phys. **92**, 5749 (2002).
[8]J. Wagner, M. Peter, K. Winkler, and K. H. Bachem, J. Appl. Phys. **83**, 4299 (1998).
[9]H. A. McKay, R. M. Feenstra, P. J. Poole, and G. C. Aers, J. Cryst. Growth **249**, 237 (2003).
[10]K. Streubel, V. Harle, F. Scholz, M. Bode, and M. Grundmann, J. Appl. Phys. **71**, 3300 (1992).
[11]P. E. Smith, S. H. Goss, S. T. Bradley, M. K. Hudait, Y. Lin, S. A. Ringel, and, L. J. Brillson, J. Vac. Sci. Technol. B **22**, 555 (2004).
[12]M. K. Hudait, Y. Lin, S. H. Goss, P. Smith, S. Bradley, L. J. Brillson, S. W. Johnston, R. K. Ahrenkiel, and S. A. Ringel (unpublished).
[13]K. Mahalingam, Y. Naamura, N. Otsuka, H. Y. Lee, M. J. Hafich, and G. Y. Robinson, J. Electron. Mater. **21**, 129 (1992).
[14]Y. K. Fukai, F. Hyuga, T. Nittono, K. Watanabe, and H. Sugahara, J. Vac. Sci. Technol. B **17**, 2524 (1999).
[15]Y. Sakai, M. Kudo, and C. Nielsen, J. Vac. Sci. Technol. A **19**, 1139 (2001).
[16]J. Van Laar and A. Huijser, J. Vac. Sci. Technol. **13**, 769 (1976).
[17]B. Kaestner, C. Schönjahn, and C. J. Humphreys, Appl. Phys. Lett. **84**, 2109 (2004).
[18]S. L. Elliott, R. F. Broom, and C. J. Humphreys, J. Appl. Phys. **91**, 9116 (2002).
[19]D. Venables, H. Jain, and D. C. Collins, J. Vac. Sci. Technol. B **16**, 362 (1998).
[20]O. Wada and H. Hasegawa, *InP-Based Materials and Devices: Physics and Technology*, 1st ed. (J. Wiley, New York, 1999), p. 83.
[21]P. Hovington, D. Drouin, and R. Gauvin, Scanning **19**, 1 (1997).
[22]S. Hernandez, N. Blanco, I. Martil, G. Gonzalez-Diaz, R. Cusco, and L. Artus, J. Appl. Phys. **93**, 9019 (2003).
[23]J. Wagner, M. Peter, K. Winkler, and K. H. Bachem, J. Appl. Phys. **83**, 4299 (1998).
[24]S. R. Forrest, P. H. Schmidt, R. B. Wilson, and M. L. Kaplan, Appl. Phys. Lett. **45**, 1199 (1984).
[25]C. Francis, P. Boucaud, J. Y. Emery, L. Goldstein, and F. H. Julien, J. Appl. Phys. **78**, 1944 (1995).
[26]M. K. Hudait, Y. Lin, M. N. Palmisiano, C. Tivarus, J. P. Pelz, and S. A. Ringel, J. Appl. Phys. **95**, 3952 (2004).